Published in final edited form as:
Proteomics Clin Appl. 2009 November 1; 3(11): 1288–1295. doi:10.1002/prca.200900005.

Quantitative Proteomic Analysis of Ovarian Cancer Cells Identified Mitochondrial Proteins Associated with Paclitaxel Resistance

Yuan Tian[1], **Aik-Choon Tan**[2], **Xiaer Sun**[1], **Matthew T Olson**[1], **Zhi Xie**[3], **Natini Jinawath**[1], **Daniel W. Chan**[1], **Ie-Ming Shih**[1], **Zhen Zhang**[1], and **Hui Zhang**[1,*]

[1] Department of Pathology, Johns Hopkins University, Baltimore MD 21231

[2] Division of Medical Oncology, Department of Medicine, University of Colorado Denver School of Medicine, Aurora CO 80045

[3] Department of Ophthalmology, Johns Hopkins University, Baltimore, MD 21231

Abstract

Paclitaxel has been widely used as an anti-mitotic agent in chemotherapy for a variety of cancers and adds substantial efficacy as the first-line chemotherapeutic regimen for ovarian cancers. However, the frequent occurrence of paclitaxel resistance limits its function in long-term management. Despite abundant clinical and cellular demonstration of paclitaxel resistant tumors, the molecular mechanisms leading to paclitaxel resistance are poorly understood. Using genomic approaches, we have previously identified an association between a BTB/POZ gene, Nac1, and paclitaxel resistance in ovarian cancer. The experiments presented here have applied multiple quantitative proteomic methods to identify protein changes associated with paclitaxel resistance and Nac1 function. The SKOV-3 ovarian serous carcinoma cell line, which has inducible expression of dominant negative Nac1, was used to determine the paclitaxel treatment associated changes in the presence and absence of functional Nac1. Quantitative proteomic analyses were performed using iTRAQ labeling and mass spectrometry. Two label-free quantitative proteomic methods: LC-MS and spectral count were used to increase confidence of proteomic quantification. A total of 1371 proteins were quantified by at least one of the quantitative proteomic methods. Candidate proteins related to paclitaxel and NAC1 function were identified in this study. Go analysis of the protein changes identified upon paclitaxel resistance revealed that cell component enrichment related to mitochondria. Moreover, tubulin and mitochondrial proteins were the major cellular components with changes associated with paclitaxel treatment. This suggests that mitochondria may play a role in paclitaxel resistance.

Keywords

ovarian cancer; paclitaxel; Taxol; mass spectrometry; proteomics

1. Introduction

Paclitaxel (Taxol®) is a potent antimitotic agent which is currently employed for the treatment of many human cancers and as an inflammation deterrent in drug-eluting cardiovascular stents

*Requests for reprints: Dr. Hui Zhang, Department of Pathology, Johns Hopkins University, 1550 Orleans Street, CRBII, Room 3M-03, Baltimore, MD 21231, hzhang32@jhmi.edu, Tel: 410-502-8149.

The authors have declared no conflict of interest.

[1]. Paclitaxel is known to induce cytotoxicity by preventing tubulin depolymerization during the metaphase to anaphase transition of mitosis [2,3] or by triggering apoptosis through regulating the expression of apoptosis-related proteins in both the caspase-dependent and caspase-independent pathways [1]. Unfortunately, while paclitaxel causes initial remission of ovarian cancer, the tumor often acquires resistance and recurs [4]. The molecular mechanisms underlying paclitaxel resistance remain unclear. The experiments presented here attempt to identify the proteins associated with paclitaxel resistance in ovarian cancer cells in order to facilitate the elucidation of molecular mechanisms of paclitaxel induced apoptosis and acquired resistance and discovery of potential drug targets for ovarian cancer with paclitaxel resistance.

Nac1, a member of BTB/POZ gene family, is a transcription repressor that is essential for the growth and survival of tumor cells [5]. We have previously associated Nac1 overexpression with tumor recurrence and paclitaxel resistance in ovarian serous carcinoma [5,6]. However, the function of Nac1 for paclitaxel resistance is not well understood. To explore this function, we generated the SKOV-3 N130 cell line which is an ovarian serous carcinoma cell line (SKOV-3) with stable transfection of N130/EGFP controlled by tTA (tetracycline-controlled transactivator) [5]. This Tet-OFF inducible system can trigger the expression of N130 by removal of doxycycline which inhibits the function of Nac1.

The relationships between paclitaxel resistance and Nac1 were explored here using iTRAQ (isoabaric tags for relative and absolute quantitation) quantitation method, and also measured by label-free quantitation methods, LC-MS and spectral count. The three methods are among the several high throughput quantitative proteomic methods that have been developed in the past decade. Method development in this field has occurred in two directions: label-dependent and label-free. The label-dependent methods are widely used and include derivitizing methods [7] such as isotope-coded affinity tags (ICAT) [8] and isobaric tags for relative and absolute quantitation (iTRAQ) [9] and non-derivitizing methods such as stable isotope labeling with amino acids in cell culture (SILAC) [10] and ^{18}O labeling [11]. When applied to proteomics, stable isotope labeling allows for the accurate measurement of the relative peptide abundance by direct comparison of light and heavy peptides in the same spectrum.

While label-dependent methods comprise the gold standard for quantitative techniques, only a limited number of samples can be quantified using isotopic derivitization in a single experiment due to the fixed number of channels from the labeling reagents. Thus an alternative direction of method development for quantitative proteomics, that of label-free quantitation methods, has evolved and includes the liquid chromatography-mass spectrometry (LC-MS) method [12,13] and spectral count [14]. The LC-MS method determines the peptide abundance by comparing the intensity of the same peptide peak in multiple LC-MS runs. Quantitation of protein abundance by spectral count is based on the number of redundant spectra acquired for each protein from different samples in the LC-MS/MS analyses. Label-free quantitative methods are theoretically capable of quantifying an unlimited number of samples in a single study. The limitation of the label-free quantitative method is that the quantitation accuracy relies heavily on the reproducible analyses of different samples in multiple LC-MS and LC-MS/MS analyses [15–18].

Therefore, it is clear that a high-throughput quantitative proteomic method has the potential to identify a large number of protein changes but that these measurements must be validated. The validation of these protein changes with traditional methods such as Western blots or immunohistochemistry is limited due to the availability, expense of the antibodies, and the low throughput of the assays. Therefore, the proteomics study should give the more confident ones for the further immune based validation. The study presented here identified protein changes related to paclitaxel resistance and Nac1 function using most reliable quantitation, iTRAQ

labeling. In addition, the two label-free quantitative proteomic methods were used to increase the quantification confidence.

Using the iTRAQ quantitation, most of these changed proteins related to paclitaxel treatment were significantly overrepresented in mitochondria. Our results suggest a new role of mitochondria of ovarian cancer cells in paclitaxel resistance and define potential new targets for treatment of paclitaxel-resistant ovarian cancer. Most protein changes in mitochondria were also identified as up-regulated by the two label-free methods. In addition, we also list the candidate proteins related to NAC1 function.

2 Materials and methods

2.1 Materials

Sequencing grade trypsin was from Promega (Madison, WI); C18 Sep-Pak Vac columns were from Waters (Milford, MA); α-cyano-4-hydroxycinnasmic acid (CHCA) was from Agilent (Palo Alto, CA); iTRAQ reagent and mass calibration standards were from Applied Biosystems (Foster City, CA); BCA assay kit was from Pierce (Rockford, IL); SCX columns and C18 resin were from Sepax (Newark, DE).; Other chemicals were purchased from Sigma-Aldrich (St. Louis, MO).

2.2 Treatments of ovarian cancer cells

The N130-inducible SKOV-3 ovarian cancer cell line, stably expressed the inducible construct of N-terminal 130 amino acids (N130) of Nac1 gene and enhanced green fluorescent protein (EGFP), was generated and reported previously [5,6]. N130-inducible SKOV-3 cells were cultured in G400D2 medium (RPMI medium contained 10% FBS, 1% penicillin/streptomycin, 400 μg/ml geneticin, and 2 μg/ml doxycycline). To induce the expression of N130, the cells were washed with PBS twice and cultured in G400 medium (G400D2 medium without doxycycline). Expression of N130-EGFP was confirmed by fluorescent microscope after 28-hour culture in G400 medium.

The N130-inducible SKOV-3 ovarian adenocarcinoma cells with and without N130 expression by culturing in two different medium as described above, were un-treated or treated with 20nM paclitaxel for 72-hour. The cells that remained alive after paclitaxel treatment were harvested at the end of paclitaxel treatment.

2.3 Peptide extraction

The cell pallets were collected and sonicated. Protein concentration was measured by BCA assay. The same amounts of proteins (1 mg) from each condition were denatured in 8M urea in 0.4M NH_4HCO_3, 0.1% (w/v) SDS solution (pH8.3), and 10mM TCEP (Tris (2-carboxythyl) phosphine) by incubation at 60°C for 1 hour. Proteins were alkylated with 16mM iodoacetamide by incubation at room temperature in the dark for 30 min. The sample was diluted 4-fold by trypsin digestion buffer (100mM NH_4HCO_3, pH8.3). Trypsin was added at a 1 to 50 part sample protein excess and allowed to digest at 37°C overnight. SDS-PAGE and silver staining was employed to ensure the completion of tryptic digest. The peptides were purified with C18 Sep-Pak Vac columns and resuspended in water with a final concentration of 10μg/μl.

2.4 iTRAQ labeling

Tryptic peptides (50 μg) from each sample were mixed with 20 μl of dissolution buffer provided with iTRAQ kit. The iTRAQ 4-plex reagents were dissolved in 70μl of methanol respectively and strongly vortexed. Each iTRAQ labeling reagent was then added to the sample and mixed.

The mixture was incubated at room temperature for 1 hour followed by cleaning up by SCX column.

2.5 Mass spectrometry analysis

For protein quantification by spectral count, each peptide mixture was analyzed twice by the LTQ ion trap mass spectrometer (Thermo Finnigan, San Jose, CA). For protein identification and quantitative analysis using LC-MS, an ESI-QSTAR mass spectrometer (Applied Biosystems, Foster City, CA) was used. In both systems, 2 μl (2 μg) peptides were injected into a peptide cartridge packed with C18 resin, and then passed through a 10 cm × 75 μm i.d. microcapillary HPLC (μLC) column packed with C18 resin. The effluent from the μLC column entered an electrospray ionization source in which peptides were ionized and passed directly into the mass spectrometers. A linear gradient of acetonitrile from 5%–32% over 100 min at flow rate of ~300 nL/min was applied. During the LC-MS mode, data was acquired in the *m/z* range of 400 and 2000. The MS/MS was also turned on to collect CID using data dependent mode. Each sample was analyzed three times by QSTAR to increase the accuracy of quantification.

iTRAQ labeled peptide was analyzed by both QSTAR and 2-D LC (Nano, Eksigent, Dublin, CA) MALDI TOF/TOF (ABI 4800, Applied Biosystems, Foster City, CA). The analysis on the QSTAR was performed in the same setting as described above. For the analysis by 2-D Nano LC and MALDI 4800-TOF/TOF, on-line integration of 15-cm-long 300μm strong cation exchange column (SCX) with 15-cm-long 300 μm of C18-reverse phase liquid chromatography (RPLC) was employed. Four SCX fractions of 0, 5, 50 and 500mM KCl and 3–45% linear acetonitrile gradient (containing 0.1% TFA and acetonitrile) of RPLC for each fraction were applied before analysis by MALDI-TOF/TOF. Peptides eluted from columns were directly mixed with CHCA and spotted on a MALDI target plate with 768 spots followed by analysis with MS and MS/MS using the ABI 4800 MALDI-TOF/TOF.

2.6 Peptide identifications

The iTRAQ data analyzed either by QSTAR or MALDI and label-free data from LTQ were searched by ProteinPilot™ software 2.0 [19] against the human International Protein Index database (IPI, version 2.28) using the cut-off probability score of 0.9.

Tandem MS spectra of label-free peptides from the QSTAR were searched with SEQUEST [20] against the same human IPI protein database (version 2.28). The peptide mass tolerance is 2.0Da. Other parameters of database searching are modified as following: cysteine modification (add cysteine 57) and oxidized methionine (add methionine with 16 Da). The output files were evaluated by INTERACT [21] and ProteinProphet [22]. The cutoff of ProteinProphet analysis is the probability score ≥ 0.9 so that low probability protein identifications can be filtered out. For each identified peptide, peptide sequence, protein name, precursor m/z value, peptide mass, charge state, retention time where the MS/MS was acquired, and probability of the peptide identification being correct were recorded and outputted using INTERACT [21].

2.7 Quantitative proteomic analyses

The ratio of the four channels of iTRAQ labeling was determined by the ProteinPilot™ software.

A suite of software tools of SpecArray were used to analyze the LC-MS data as described previously [23]. For each peptide peak, an abundance ratio of matched peptides in different samples was determined for each peptide peak. An in-house Perl script was then used to link

the peptide identification from MS/MS spectra to their corresponding MS peaks by matching precursor mass within 1 Da, retention time within 10 min, and charge state of the peptides.

The identified peptides from LTQ with a probability score ≥ 0.9 were used for the spectral count. To determine the number of MS/MS spectra used for identification of each protein in different conditions using our in-house developed software tool. For peptide sequence that could come from multiple proteins, the spectral count is equally distributed to all proteins with the identified peptide. Due to random sampling of mass spectrometer in collecting MS/MS spectra used for spectral count, we only quantified proteins with at least 4 spectral counts in total from the four cell states.

2.8 Evaluation of the cut-off of protein abundance ratio for proteins changes

To correct for any systematic errors of protein ratio introduced by sample handling and to determine the appropriate cut-off for protein changes, the distribution of abundance ratios in different cell states was generated for each quantitative method. Since the majority of proteins were not expressed differently in two cell states, we normalized the ratio based on the distribution of the protein abundance ratios from two cell states. Proteins fell out of the normal distribution from the abundance ratio of two cell states were considered as altered proteins. The threshold to select protein changes was based on the ratio distribution of two cell states. The mean and standard deviation of ratio from two cell states were calculated, and the abundance of proteins with an abundance ratio outside of one standard deviation from the mean were flagged as altered.

2.9 Cellular component classification of changed genes

To classify the changed proteins into cellular component, GO (Gene Ontology) [24] analysis (http://www.godatabase.org/dev) was performed. All the identified and quantified proteins by iTRAQ quantitation were used as background. Protein changes due to paclitaxel quantified by iTRAQ were used as changed proteins. P value was calculated using one-side Fisher exact test. To correct for multiple testing errors, p value was adjusted the minimum P method of Westfall and Young[25].

3 Results and discussion

3.1 Inducible expression of N130 in SKOV-3 cells

To identify proteins related to paclitaxel treatment and resistance, SKOV-3 cells with inducible expression of N130 protein [6,26] was used in this study. The quantitative proteomic analyses of paclitaxel treatment for SKOV-3 N130 cells with and without expression of N130 are schematically illustrated in Figure 1 and consist of four steps: 1) two dishes were treated to induce the expression of N130 and two dishes were untreated as controls; 2) One dish with expression of N130 and one dish without expression of N130 were treated with paclitaxel, and the other two dishes were not treated with paclitaxel act as controls; 3) the peptides were extracted from cell lysate of the four cell states by sonication and trypsin digestion; 4) the tryptic peptides were identified and quantified by iTRAQ labeling, LC-MS, and spectral count.

To evaluate the expression of N130, the florescence of EGFP was monitored as an indicator to determine whether N130 was induced after removing doxycycline from culture medium. SKOV-3 N130 cells were observed after 28-hour culture in medium with and without doxycycline according to our previous study [6,26]. The cells were observed under florescence microscope (Figure 2A and B). The induced expression of N130/EGFP by doxycycline withdrawal was indicated by the green fluorescent (Figure 2D), which was not observed in cells cultured with doxycycline (shown in Figure 2C). Thus the expression of N130 can be robustly induced in SKOV-3 N130 cells.

3.2 Quantitative proteomic analyses to identify protein changes

To determine the protein changes related to paclitaxel treatment and Nac1 function, the ovarian cancer cells with and without Nac1 function were treated with paclitaxel. After treated with 20nM paclitaxel for 72-hour, around 60 % cells was alive, which were considered as cells resistant to paclitaxel. The cells that remained alive after paclitaxel treatment were harvested at the end of paclitaxel treatment. The cell pallets were sonicated and 1 mg proteins from each cell states were digested by trypsin, followed by quantitative proteomic analysis using iTRAQ. A portion of tryptic peptides (50 μg) from N130-ON without paclitaxel treatment (ON−T), N130-ON with paclitaxel treatment (ON+T), N130-OFF without paclitaxel treatment (OFF −T) and N130-OFF with paclitaxel treatment (OFF+T) cells were labeled with 114, 115, 116 and 117 of iTRAQ reagents and analyzed by LC-MALDI TOF/TOF and LC-QSTAR for quantitative proteomic analysis. We were able to identify and quantify 850 proteins using iTRAQ labeling.

We then determined the protein changes in two cell states quantified by iTRAQ. When cells are induced of N130 expression or treated of paclitaxel, majority of cellular proteins are expected to be not affected and stay in the same level [27]. However, due to errors introduced by analytical procedures, such as sample handling and quantification process, the protein ratio from majority of proteins may be shifted. To determine the proteins with abundance changes in two cell states, histogram was used to generate the number of proteins in different abundance ratio (Figure 3). The threshold was set as < 0.7 and >1.3 for iTRAQ labeling. Majority of proteins (554 proteins, 65%) were distributed within one standard deviation (0.25) from the mean (1.046) and were considered as unchanged. Proteins that fell out of one standard deviation of the normal distribution curve were considered as with changed. A total of 296 proteins were changed due to paclitaxel treatment (160 proteins) or Nac1 inactivation (93 proteins) or both of paclitaxel treatment and Nac1 inactivation (181 proteins).

Nac1 was determined as changed upon the induced expression of N130. A total of seven peptides were identified and quantified from Nac1, and all the identified peptides were located in the N-terminus 1-130 amino acids (with 71% sequence coverage of N 130), indicating that the identified peptides were likely from overexpressed N130 instead of endogenous Nac1 protein. The amount of N130 in N130 ON cells was measured as about 10-fold higher than it in N130 OFF cells (Table 1). The quantitative results of N130 expression confirmed that: 1) the inducible Tet-OFF system was efficient in inducing N130 expression; 2) the iTRAQ quantitative methods was able to determine the relative abundance of proteins and could be used for identification of other protein changes.

3.3 Altered proteins related to Nac1 function and paclitaxel treatment

The 296 unique protein alterations determined by iTRAQ labeling were listed in Table 2 and grouped into 3 classes: 1) Protein changes upon paclitaxel treatment (OFF−T vs. OFF+T). These include proteins elevated upon paclitaxel treatment such as *tubulin beta-5 chain*, *tubulin alpha-4 chain*, mitochondrial proteins such as *cytochrome c* and *ATP synthase, mitochondrial inner membrane protein*, acute-phase proteins such as *hemoglobin*, cell surface antigens such as *CD44* and *4F2 cell surface antigen*, etc., and proteins with decreased abundance upon paclitaxel treatment such as seven subunits of *ribosomal proteins*, proteins regulating cell meiosis, mitosis and postmitotic functions such as *mitogen-activated protein kinase3*, etc. 2) Changed protein expression upon inactivation of Nac1 (OFF−T vs. ON−T). Induced expression of N130 (ON−T) inhibits the function of Nac1. Since Nac1 is a potential transcriptional repressor [26], the proteins with altered expression after Nac1 inhibition could be controlled by Nac1. These proteins include *Ras-related protein Rab-8, transcription repressor, eukaryotic translation initiation factor 3, etc*. 3) Changes of protein abundance upon paclitaxel treatment and induced N130 expression (OFF−T vs. ON+T), and proteins in this class might associate

with the function of Nac1 gene in the response to paclitaxel treatment. Proteins in this class include *Ras GTPase-activating-like protein IQGAP1, polyadenylate-binding protein 1, etc*.

Although the proteins identified in this proteomic study need further investigation to facilitate the understanding of the biological mechanism of Nac1 function or paclitaxel treatment, the results provide a list of proteins and cellular machinery, including ribosomal complexes, cell surface antigens, and stress response proteins, such as heat shock proteins and acute-phase proteins. These protein changes associated with Nac1 or paclitaxel resistance can be exploited as targets for treatment of paclitaxel resistance.

To further analyze the relationship of the protein changes upon paclitaxel treatment, the GO categories of protein changes were classified. Cellular components analysis revealed that the protein changes are significantly overrepresented in mitochondrion in the set of all proteins identified by iTRAQ (*p* value of Fisher's product: 8.8 e-5, *p* value corrected by multiple testing: 0.024).

Furthermore, we found some interesting co-regulation of tubulin and mitochondrial proteins after paclitaxel treatment. Tubulin is a well-known target for paclitaxel function and responsible for paclitaxel induced cell death [33]. One of the mechanisms of paclitaxel function is believed to induce cell death by altering microtubule assembly through the binding to the microtubule polymer so as to stabilize microtubules [34], as a result, it disrupts the normal re-assembling of microtubule network which is required by mitosis and cell proliferation [3]. Another protein, *cytochrome c*, was reported previously of release from mitochondrion thus inducing cell apoptosis upon paclitaxel treatment [35]. However, how cytochrome c was released upon paclitaxel treatment is not clear. Interestingly, in this study, both α-4 and β-5 subunit of tubulin were observed of up-regulated after paclitaxel treatment (Table 1), so were many mitochondrial proteins including *mitochondrial trifunctional enzyme, mitochondrial ATP synthase, cytochrome c, Serine hydroymethyltransferase, GrpE protein homolog 1, Mitochondrial inner membrane protein, Complement component 1 Q subcomponent binding protein, Thioredoin-dependent peroide reductase,* and *mitochondrial malate dehydrogenase*, etc.

This observation suggests a regulation of mitochondrial function associated with paclitaxel treatment and tubulins. The regulation of mitochondrial function by tubulins was also reported by several studies recently. The regulation might be the result of direct interaction of the voltage-dependent anion channel (VDAC) on mitochondrial outer membrane with tubulin [36–38]. Taken together, a hypothesis is that mitochondria may be involved in the response to paclitaxel treatment. Mitochondrial function is the key player for cell apoptosis, and the mechanism of paclitaxel treatment might be to induce apoptosis through tubulin polymerization and regulation of mitochondrial function.

3.4 protein changes determined by label-free quantitation

Quantitative analysis using different quantitative proteomic methods may increase the confidence of the protein changes if the proteins could be identified and quantified by multiple methods consistently. To this end, label free quantitation methods were also employed in this study. The tryptic peptides from the four cell states without iTRAQ labeling were analyzed three times with the QSTAR for the LC-MS quantitative analysis and two times with the LTQ for spectral count (Figure 1). A total of 383 proteins were quantified by the LC-MS method, and 757 were quantified by spectral count (Figure 4).

We then determined the proteins that were changed in two cell states quantified by LC-MS and spectral count. Similar as iTRAQ quantitation, proteins that fell out of one standard

deviation of the normal distribution curve were considered as with changed expression. The thresholds were determined as <0.75 and >1.15 for both spectral count and LC-MS.

Since N130 was induced expressed in cells, N130 was the perfect internal control for quantitation. N130 should be over-expressed in N130 ON cells compared to the N130 OFF cells. All the three quantitation showed the higher abundance of N130 in N130 ON cells (Table 1). However, the detection limitation varied among the three methods. The N130 overexpression were undetectable in N130 OFF cells for LC-MS and spectral count (Table 1), which may come from different instrumentations with various dynamic range and background. Further work and experiments will help define the most accurate quantifications along with better standards for calibrating the ratio of protein abundance from different methods. This is needed in proteomics to improve quantitative accuracy [28]. Nevertheless, the quantitative results of N130 expression confirmed that the three quantitative proteomic methods could be used to increase the confidence of quantitation.

For the mitochondria protein changes upon piclitaxel treatment, 7 out of 14 proteins determined by iTRAQ were also measured by the label free methods in the same track, e.g. ATP synthase, cytochrome c, Trifunctional enzyme, and Enoyl-CoA hydratase, etc (Table 3). Those proteins consistently determined by the two label-free methods confirmed the real changes of mitochondrial proteins upon piclitaxel treatment. This study represents the first proteomic study to discover the association of paclitaxel treatment and mitochondria protein changes in ovarian cancer cells, which may offer a new direction for studying the mechanism of drug resistance of cancer cells.

4 Concluding remarks

In this study, 1371 proteins were identified and quantified from Nac1 dominant negative model, SKOV-3 N130 cell line, associated with paclitaxel resistance and Nac1 function using iTRAQ quantitation, LC-MS method and spectral count. Candidate proteins related to paclitaxel resistance and NAC1 function were determined. Go analysis of the protein changes upon paclitaxel resistance revealed that protein changes significantly overrepresented in mitochondria. The co-regulation of tubulins and mitochondrial proteins was found, which suggests the roles of mitochondria in response to paclitaxel treatment. The identified proteins will be useful for further study of biological functions of Nac1 and elucidation of the molecular mechanism of paclitaxel treatment and resistance.

Supplementary Material

Refer to Web version on PubMed Central for supplementary material.

Acknowledgments

This work was supported by federal funds from the National Cancer Institute, National Institutes of Health, by grant R21-CA-114852 and RO1-CA-103937 (IMS) and Early Detection and Research Network (EDRN). We gratefully acknowledge the support from the Mass Spectrometry Facility at the Johns Hopkins University and the support from Applied Biosystems.

References

1. Khayat D, Antoine EC, Coeffic D. Taxol in the management of cancers of the breast and the ovary. Cancer Invest 2000;18:242–260. [PubMed: 10754992]
2. Jordan MA, Wendell K, Gardiner S, Derry WB, et al. Mitotic block induced in HeLa cells by low concentrations of paclitaxel (Taxol) results in abnormal mitotic exit and apoptotic cell death. Cancer Res 1996;56:816–825. [PubMed: 8631019]

3. Amos LA, Lowe J. How Taxol stabilises microtubule structure. Chem Biol 1999;6:R65–69. [PubMed: 10074470]
4. Sangrajrang S, Fellous A. Taxol resistance. Chemotherapy 2000;46:327–334. [PubMed: 10965098]
5. Ishibashi M, Nakayama K, Yeasmin S, Katagiri A, et al. A BTB/POZ gene, NAC-1, a tumor recurrence-associated gene, as a potential target for Taxol resistance in ovarian cancer. Clin Cancer Res 2008;14:3149–3155. [PubMed: 18483383]
6. Nakayama K, Nakayama N, Davidson B, Sheu JJ, et al. A BTB/POZ protein, NAC-1, is related to tumor recurrence and is essential for tumor growth and survival. Proc Natl Acad Sci U S A 2006;103:18739–18744. [PubMed: 17130457]
7. Zhang H, Li XJ, Martin DB, Aebersold R. Identification and quantification of N-linked glycoproteins using hydrazide chemistry, stable isotope labeling and mass spectrometry. Nat Biotechnol 2003;21:660–666. [PubMed: 12754519]
8. Gygi SP, Rist B, Gerber SA, Turecek F, et al. Quantitative analysis of complex protein mixtures using isotope-coded affinity tags. Nat Biotechnol 1999;17:994–999. [PubMed: 10504701]
9. Ross PL, Huang YN, Marchese JN, Williamson B, et al. Multiplexed protein quantitation in Saccharomyces cerevisiae using amine-reactive isobaric tagging reagents. Mol Cell Proteomics 2004;3:1154–1169. [PubMed: 15385600]
10. Ong SE, Blagoev B, Kratchmarova I, Kristensen DB, et al. Stable isotope labeling by amino acids in cell culture, SILAC, as a simple and accurate approach to expression proteomics. Mol Cell Proteomics 2002;1:376–386. [PubMed: 12118079]
11. Yao X, Freas A, Ramirez J, Demirev PA, Fenselau C. Proteolytic 18O labeling for comparative proteomics: model studies with two serotypes of adenovirus. Anal Chem 2001;73:2836–2842. [PubMed: 11467524]
12. Bondarenko PV, Chelius D, Shaler TA. Identification and relative quantitation of protein mixtures by enzymatic digestion followed by capillary reversed-phase liquid chromatography-tandem mass spectrometry. Anal Chem 2002;74:4741–4749. [PubMed: 12349978]
13. Chelius D, Bondarenko PV. Quantitative profiling of proteins in complex mixtures using liquid chromatography and mass spectrometry. J Proteome Res 2002;1:317–323. [PubMed: 12645887]
14. Liu H, Sadygov RG, Yates JR 3rd. A model for random sampling and estimation of relative protein abundance in shotgun proteomics. Anal Chem 2004;76:4193–4201. [PubMed: 15253663]
15. Zhang H, Yi EC, Li XJ, Mallick P, et al. High throughput quantitative analysis of serum proteins using glycopeptide capture and liquid chromatography mass spectrometry. Mol Cell Proteomics 2005;4:144–155. [PubMed: 15608340]
16. Olson MT, Blank PS, Sackett DL, Yergey AL. Evaluating reproducibility and similarity of mass and intensity data in complex spectra--applications to tubulin. J Am Soc Mass Spectrom 2008;19:367–374. [PubMed: 18207417]
17. Frewen BE, Merrihew GE, Wu CC, Noble WS, MacCoss MJ. Analysis of peptide MS/MS spectra from large-scale proteomics experiments using spectrum libraries. Anal Chem 2006;78:5678–5684. [PubMed: 16906711]
18. Lam H, Deutsch EW, Eddes JS, Eng JK, et al. Development and validation of a spectral library searching method for peptide identification from MS/MS. Proteomics 2007;7:655–667. [PubMed: 17295354]
19. Shilov IV, Seymour SL, Patel AA, Loboda A, et al. The Paragon Algorithm, a next generation search engine that uses sequence temperature values and feature probabilities to identify peptides from tandem mass spectra. Mol Cell Proteomics 2007;6:1638–1655. [PubMed: 17533153]
20. Eng JM, AL, Yates JR 3rd. An approach to correlate tandem mass spectral data of peptides with amino acid sequences in a protein database. J Am Soc Mass Spectrom 1994;5:13.
21. Han DK, Eng J, Zhou H, Aebersold R. Quantitative profiling of differentiation-induced microsomal proteins using isotope-coded affinity tags and mass spectrometry. Nat Biotechnol 2001;19:946–951. [PubMed: 11581660]
22. Keller A, Nesvizhskii AI, Kolker E, Aebersold R. Empirical statistical model to estimate the accuracy of peptide identifications made by MS/MS and database search. Anal Chem 2002;74:5383–5392. [PubMed: 12403597]

23. Li XJ, Yi EC, Kemp CJ, Zhang H, Aebersold R. A software suite for the generation and comparison of peptide arrays from sets of data collected by liquid chromatography-mass spectrometry. Mol Cell Proteomics 2005;4:1328–1340. [PubMed: 16048906]
24. Ashburner M, Ball CA, Blake JA, Botstein D, et al. Gene ontology: tool for the unification of biology. The Gene Ontology Consortium. Nat Genet 2000;25:25–29. [PubMed: 10802651]
25. Westfall, PaYS. Resampling-Based Multiple Testing: Examples and Methods for p-Value Adjustment. 1993.
26. Nakayama K, Nakayama N, Wang TL, Shih Ie M. NAC-1 controls cell growth and survival by repressing transcription of Gadd45GIP1, a candidate tumor suppressor. Cancer Res 2007;67:8058–8064. [PubMed: 17804717]
27. Li XJ, Zhang H, Ranish JA, Aebersold R. Automated statistical analysis of protein abundance ratios from data generated by stable-isotope dilution and tandem mass spectrometry. Anal Chem 2003;75:6648–6657. [PubMed: 14640741]
28. Lau KW, Jones AR, Swainston N, Siepen JA, Hubbard SJ. Capture and analysis of quantitative proteomic data. Proteomics 2007;7:2787–2799. [PubMed: 17640002]
29. Li Y, Sokoll LJ, Rush J, Zou N, Chan DW. Targeted detection of prostate cancer proteins in serum using heavy peptide standards and MALDI-TOF/TOF. Proteomics-Clinical Applications. 2009 In press.
30. Stahl-Zeng J, Lange V, Ossola R, Eckhardt K, et al. High sensitivity detection of plasma proteins by multiple reaction monitoring of N-glycosites. Mol Cell Proteomics 2007;6:1809–1817. [PubMed: 17644760]
31. Keshishian H, Addona T, Burgess M, Kuhn E, Carr SA. Quantitative, multiplexed assays for low abundance proteins in plasma by targeted mass spectrometry and stable isotope dilution. Mol Cell Proteomics 2007;6:2212–2229. [PubMed: 17939991]
32. Anderson L, Hunter CL. Quantitative mass spectrometric multiple reaction monitoring assays for major plasma proteins. Mol Cell Proteomics 2006;5:573–588. [PubMed: 16332733]
33. Umezu T, Shibata K, Kajiyama H, Terauchi M, et al. Taxol resistance among the different histological subtypes of ovarian cancer may be associated with the expression of class III beta-tubulin. Int J Gynecol Pathol 2008;27:207–212. [PubMed: 18317222]
34. Orr GA, Verdier-Pinard P, McDaid H, Horwitz SB. Mechanisms of Taxol resistance related to microtubules. Oncogene 2003;22:7280–7295. [PubMed: 14576838]
35. Kuo HC, Lee HJ, Hu CC, Shun HI, Tseng TH. Enhancement of esculetin on Taxol-induced apoptosis in human hepatoma HepG2 cells. Toxicol Appl Pharmacol 2006;210:55–62. [PubMed: 16051289]
36. Rostovtseva TK, Sheldon KL, Hassanzadeh E, Monge C, et al. Tubulin binding blocks mitochondrial voltage-dependent anion channel and regulates respiration. Proc Natl Acad Sci U S A 2008;105:18746–18751. [PubMed: 19033201]
37. Carre M, Andre N, Carles G, Borghi H, et al. Tubulin is an inherent component of mitochondrial membranes that interacts with the voltage-dependent anion channel. J Biol Chem 2002;277:33664–33669. [PubMed: 12087096]
38. Rostovtseva TK, Bezrukov SM. VDAC regulation: role of cytosolic proteins and mitochondrial lipids. J Bioenerg Biomembr 2008;40:163–170. [PubMed: 18654841]

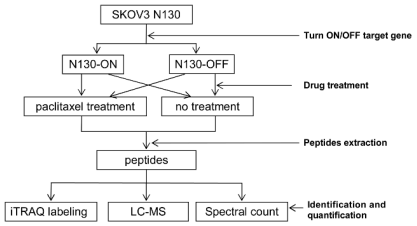

Figure 1.
Flowchart of the quantitative study of Nac1 function and paclitaxel treatment

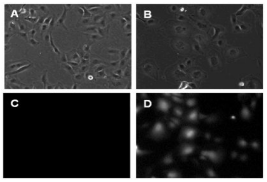

Figure 2.
Expression of fusion protein N130-EGFP in SKOV-3 ovarian cell line: A) SKOV-3 N130 cultured with doxycycline, the N130-EGFP expression was off; B) SKOV-3 N130 cultured without doxycycline, the N130-EGFP expression was on; C) no fluorescent came from SKOV-3 N130 cultured with doxycycline; D) fluorescent came from SKOV-3 N130 cultured without doxycycline.

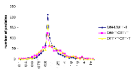

Figure 3.
The histogram analysis of peptide ratios of different cell states quantified by iTRAQ

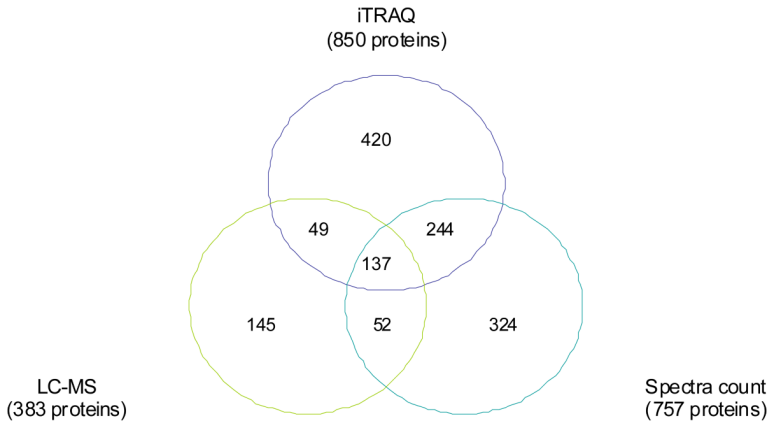

Figure 4.
Venn diagram depicts the number of proteins quantified by each quantitation method

Table 1

Overexpression of N130 determined by three quantitative proteomic methods. For iTRAQ quantitation, all ratios are normalized to the reporter ion at m/z 116 (OFF-T). For LC-MS quantitation, the number showed the peak intensities.

Methods	OFF−T	OFF+T	ON−T	ON+T
iTRAQ	1.00	1.08±0.41	10.73±2.87	12.13±5.21
LC-MS	0.00±0.00	0.00±0.00	2628.84±167.78	3244.69±335.38
Spectral count	0.00	5.00	80.13	83.00

Table 2

Proteins associated with paclitaxel treatment with and without N130 overexpression determined by iTRAQ

IPI	ProteinName	Swiss-Prot	% Cov	OFF+T/OFF−T	ON−T/OFF−T	ON+T/OFF−T
Proteins regulated upon paclitaxel treatment						
IPI00298971	Vitronectin (S-protein) (V75)	P04004	3.1	2.54	1.44	2.50
IPI00328696	Hemoglobin alpha chain	P01922	21.2	2.45	1.20	2.78
IPI00305185	Stromal cell protein	Q9BRV3	10.9	2.37	1.67	3.15
IPI00028481	Ras-related protein Rab-8	P24407	12.1	2.32	3.32	2.16
IPI00160897	Hypothetical protein	Q969E5	37.6	2.05	1.08	2.27
IPI00396589	Interleukin enhancer binding factor 2, 45kD	Q9BWD4	11.5	2.01	0.88	1.63
IPI00026087	Barrier-to-autointegration factor	O75531	15.7	1.84	2.47	
IPI00299149	Ubiquitin-like protein SMT3B	P55855	32.6	1.83	1.48	1.08
IPI00218816	beta globin	P02023	19.7	1.81	2.10	2.49
IPI00219219	beta-galactosidase binding lectin	P09382	65.2	1.81	1.14	1.39
IPI00030131	Splice isoform Beta of P42167 Thymopoietin, isoforms beta/gamma	P42167	14.1	1.81	1.23	2.11
IPI00009346	Protein C6orf53	Q9P0S9	13.4	1.80		
IPI00002520	Serine hydroymethyltransferase, mitochondrial	P34897	12.5	1.79	1.13	1.34
IPI00013452	Bifunctional aminoacyl-tRNA synthetase	P07814	4.2	1.78	1.30	1.28
IPI00027192	Procollagen-lysine,2-ooglutarate 5-dioygenase 1	Q02809	3.9	1.77	2.10	0.84
IPI00329705	KIAA1363 protein	Q86WZ1	9.8	1.76	1.18	2.77
IPI00374657	vesicle-associated membrane protein-associated protein A isoform 1		4.9	1.74	1.49	0.97
IPI00236879	Atain-2 related domain protein	Q8WWM7	7.1	1.74	1.51	1.84
IPI00219291	ATP synthase f chain, mitochondrial	P56134	37.9	1.73	1.15	1.73
IPI00015786	Spectrin alpha chain, brain	Q13813	11.2	1.71	1.41	1.89
IPI00382733	Transcription repressor	O75799	6.6	1.68	1.84	1.19
IPI00025273	Trifunctional purine biosynthetic protein adenosine-3	P22102	10.1	1.68	1.43	1.57
IPI00006558	CGI-61 protein	Q9NR47	10.1	1.67	1.32	0.75
IPI00011229	Cathepsin D	P07339	14.1	1.66	1.02	1.61
IPI00305064	CD44	P16070	6.3	1.65	1.26	1.65
IPI00025874	Dolichyl-diphosphooligosaccharide--protein glycosyltransferase 67 kDa subunit	P04843	15.7	1.65	1.20	1.48

IPI	ProteinName	Swiss-Prot	% Cov	OFF+T/OFF−T	ON−T/OFF−T	ON+T/OFF−T
IPI00029557	GrpE protein homolog 1, mitochondrial	Q9HAV7	18.4	1.65	1.30	1.46
IPI00290889	DNA topoisomerase I	P11387	2.4	1.64	1.01	1.27
IPI00009960	Mitochondrial inner membrane protein	Q16891	7.4	1.64	1.20	1.05
IPI00218682	P13674 Prolyl 4-hydroylase alpha-1 subunit	P13674	5.4	1.62	0.82	1.21
IPI00015148	Ras-related protein Rap-1b	P09526	14.7	1.61	1.11	1.44
IPI00215916	cytochrome c	P00001	29.5	1.61	1.21	1.73
IPI00016572	Small nuclear ribonucleoprotein G	Q15357	17.1	1.60	1.52	1.77
IPI00218019	Basigin long isoform	Q8IZL7	9.6	1.59	0.84	1.57
IPI00005202	Membrane associated progesterone receptor component 2	O15173	10.3	1.59	1.14	2.17
IPI00009236	Caveolin-1	Q03135	24.2	1.56	1.22	1.66
IPI00019472	Neutral amino acid transporter B(0)	Q15758	7.4	1.55	0.68	1.19
IPI00031522	Trifunctional enzyme alpha subunit, mitochondrial	P40939	4.7	1.55	0.80	1.19
IPI00216492	P31942 Heterogeneous nuclear ribonucleoprotein H3	P31942	10.9	1.55	1.14	1.35
IPI00219835	P04895 Guanine nucleotide-binding protein G(S), alpha subunit	P04895	23.9	1.55	1.06	1.64
IPI00016447	Hypothetical protein FLJ20502	Q9N08	13.1	1.53	1.08	2.08
IPI00220739	progesterone receptor membrane component 1	O00264	27.7	1.52	1.08	1.42
IPI00025019	Proteasome subunit beta type 1	P20618	21.2	1.52	1.00	0.64
IPI00217952	Glucosamine--fructose-6-phosphate aminotransferase [isomerizing] 1	Q06210	8.6	1.51	0.96	1.52
IPI00014238	Lysyl-tRNA synthetase	Q15046	6.7	1.50	1.49	
IPI00385566	Hypothetical protein FLJ30014	Q969M3	3.5	1.50	1.62	1.56
IPI00300074	Phenylalanyl-tRNA synthetase beta chain	Q9NSD9	10.7	1.48	1.17	0.97
IPI00141318	P63 protein	Q07065	17.6	1.47	1.07	1.25
IPI00142634	Tubulin beta-5 chain	P05218	43	1.47	1.00	1.47
IPI00017726	3-hydroyacyl-CoA dehydrogenase type II	Q99714	15.3	1.47	1.04	1.74
IPI00014230	Complement component 1, Q subcomponent binding protein, mitochondrial	Q07021	19.9	1.47	1.17	1.25
IPI00005159	Actin-like protein 2	O15142	19.3	1.47	1.22	1.00
IPI00107117	Peptidylprolyl isomerase B	P23284	25.9	1.47	1.32	1.72
IPI00024911	Endoplasmic reticulum protein ERp29	P30040	5	1.46	1.10	1.27
IPI00220985	Keratin, type I cytoskeletal 18	P05783	39.6	1.46	0.94	1.49
IPI00180128	Similar to KIAA0005 gene product	Q9BUY0	10.4	1.45	1.11	1.29

IPI	ProteinName	Swiss-Prot	% Cov	OFF+T/OFF−T	ON−T/OFF−T	ON+T/OFF−T
IPI00383671	serologically defined breast cancer antigen 84 isoform a	Q9Y282	7.2	1.45	1.21	1.10
IPI00395917	ferritin heavy chain	P02794	14.8	1.44	0.87	1.87
IPI00374410	cytochrome b5 reductase soluble isoform	P003781-2	26.6	1.43	0.90	1.26
IPI00031479	Protein disulfide isomerase A5	Q14554	2.3	1.43	0.88	1.54
IPI00028055	Transmembrane protein Tmp21	P49755	22.4	1.41	1.11	1.32
IPI00303882	Cargo selection protein TIP47	O60664	27.2	1.41	1.26	1.60
IPI00384489	Similar to adaptor-related protein comple 1, beta 1 subunit	Q10567	8.7	1.41	1.14	1.24
IPI00021766	Splice isoform 1 of Q9NQC3 Reticulon 4	Q9NQC3	7.1	1.41	1.09	1.32
IPI00011937	Peroiredoin 4	Q13162	17.7	1.41	1.73	
IPI00003965	Ubiquitin carboyl-terminal hydrolase 7	Q93009	1.9	1.40	1.08	1.65
IPI00024919	Thioredoin-dependent peroide reductase, mitochondrial	P30048	25.4	1.40	1.05	1.39
IPI00386755	ERO1 (S. cerevisiae)-like	Q96HE7	3	1.39	1.06	1.21
IPI00219604	mitogen-activated protein kinase kinase 1	Q02750	7.6	1.39	0.99	1.36
IPI00009407	Defender against cell death 1	P46966	14.2	1.39	1.13	1.94
IPI00004902	Electron transfer flavoprotein beta-subunit	P38117	14.1	1.38	1.03	1.06
IPI00024993	Enoyl-CoA hydratase, mitochondrial	P30084	14.1	1.38	0.81	1.12
IPI00046828	similar to CG15881-PB	Q4VC31	14.5	1.37		1.33
IPI00021954	Golgi-specific brefeldin A-resistance guanine nucleotide echange factor 1	Q92538	7	1.37	0.87	1.43
IPI00165092	Hypothetical protein FLJ13995	Q9H817	6.3	1.37	0.87	1.61
IPI00027493	4F2 cell-surface antigen heavy chain	P08195	22.9	1.37	0.97	1.36
IPI00007750	Tubulin alpha-4 chain	P05215	40	1.37	1.04	1.29
IPI00009329	Utrophin	P46939	1.3	1.37	1.44	0.92
IPI00216393	Splice isoform Non-brain of P09496 Clathrin light chain A	P09496	9.6	1.37	1.37	1.09
IPI00337814	Hypothetical protein	Q9BWL4	11.7	1.37	1.16	1.65
IPI00026167	NHP2-like protein 1	P55769	24.2	1.37	0.86	1.46
IPI00396321	Hypothetical protein	Q9P189	25.7	1.36	1.00	1.17
IPI00386621	Similar to calmodulin 2	Q9BRL5	16.3	1.36	1.44	1.10
IPI00029574	Putative S100 calcium-binding protein A11 pseudogene	O60417	10.8	1.36	0.85	1.26
IPI00027423	Serine/threonine protein phosphatase PP1-alpha 1 catalytic subunit	P08129	10.6	1.36	1.07	1.05
IPI00007682	Vacuolar ATP synthase catalytic subunit A, ubiquitous isoform	P38606	6.3	1.35	0.90	1.07

Proteomics Clin Appl. Author manuscript; available in PMC 2010 November 22.

IPI	ProteinName	Swiss-Prot	% Cov	OFF+T/OFF−T	ON−T/OFF−T	ON+T/OFF−T
IPI00160021	HIRA-interacting protein 5	Q9UMS0	10.2	1.35	1.17	1.10
IPI00291005	cytosolic malate dehydrogenase	P40925	9.9	1.34	0.46	0.95
IPI00007928	PRP8 protein	O14547	6.2	1.34	1.02	0.96
IPI00220834	ATP-dependant DNA helicase II	P13010	14.1	1.34	1.38	0.91
IPI00016513	Ras-related protein Rab-10	O88386	8	1.34	1.07	1.18
IPI00009950	Vesicular integral-membrane protein VIP36	Q12907	6.7	1.34	0.92	1.17
IPI00029079	GMP synthase [glutamine-hydrolyzing]	P49915	9.6	1.33	2.70	2.50
IPI00297084	Dolichyl-diphosphooligosaccharide--protein glycosyltransferase 48 kDa subunit	P39656	12.7	1.33	1.32	1.41
IPI00290142	CTP synthase	P17812	12.5	1.33	1.10	1.42
IPI00009922	DC50	Q9GZT3	12.8	1.33	1.01	1.42
IPI00006865	Vesicle trafficking protein SEC22B	O75396	11.2	1.33	1.61	
IPI00293102	Splice isoform 2 of Q15257 Protein phosphatase 2A, regulatory subunit B′	Q15257	12.8	1.33	1.05	1.45
IPI00008240	Methionyl-tRNA synthetase	P56192	7.8	1.33	1.09	1.20
IPI00220855	Similar to H2A histone family, member O	Q9BTM1	58.9	1.33	0.89	1.42
IPI00186338	unnamed protein		41.9	1.33	1.09	1.30
IPI00329351	60 kDa heat shock protein, mitochondrial	P10809	31	1.33	1.05	1.31
IPI00007765	Stress-70 protein, mitochondrial	P38646	28.4	1.33	1.05	1.12
IPI00026328	Thioredoin-like protein p19	O95881	5.2	1.33	1.30	1.32
IPI00027434	Transforming protein RhoC	P08134	19.7	1.32	1.22	1.09
IPI00005270	Hypothetical protein	Q9BVD2	1.8	1.32	2.46	1.41
IPI00003815	Rho GDP-dissociation inhibitor 1	P52565	16.7	1.32	0.97	1.22
IPI00024364	Importin beta-2 subunit	Q92973	7.3	1.31	0.61	1.21
IPI00006482	Sodium/potassium-transporting ATPase alpha-1 chain	P05023	10.8	1.31	1.31	1.33
IPI00021785	Cytochrome c oidase polypeptide Vb, mitochondrial	P10606	25.6	1.31	1.38	2.03
IPI00304802	Dihydrolipoamide succinyltransferase component of 2-ooglutarate dehydrogenase comple, mitochondrial	P36957	11.9	1.31	0.92	1.23
IPI00027252	repressor of estrogen receptor activity	Q9BV3	15.1	1.31	0.96	1.54
IPI00328188	fatty acid synthase	Q96IT0	9.8	1.31	0.96	1.11
IPI00027717	Component of gems 4	P57678	4.6	1.30	1.17	1.76
IPI00022793	Trifunctional enzyme beta subunit, mitochondrial	P55084	13.5	1.30	1.29	1.35

IPI	ProteinName	Swiss-Prot	% Cov	OFF+T/OFF−T	ON−T/OFF−T	ON+T/OFF−T
IPI00021978	Peroisome assembly factor	O96011	6.2	1.30	0.77	0.78
IPI00008167	Sodium/potassium-transporting ATPase beta-3 chain	P54709	10.4	1.30	0.96	1.26
IPI00334713	Heterogeneous nuclear ribonucleoprotein A/B	Q99729	21.4	0.69	0.00	1.21
IPI00219158	ribosomal protein L29	P47914	30.8	0.69	1.17	0.53
IPI00033904	similar to ribosomal protein S3a	P61247	26.5	0.69	1.03	0.63
IPI00004860	Arginyl-tRNA synthetase	P54136	6.8	0.69	1.02	0.88
IPI00219446	prostatic binding protein	P30086	20.3	0.68	0.43	0.54
IPI00374260	ribosomal protein L10	P27635	30.4	0.68	0.98	0.69
IPI00052229	Hypothetical protein	Q9UG74	6.7	0.68	0.98	2.48
IPI00005680	Hypothetical protein KIAA0095	Q14705	6.2	0.68	1.48	0.73
IPI00385244	phosphoglycerate mutase 1 (brain)	P18669	23.2	0.68	1.15	1.20
IPI00002149	GTP-binding protein SAR1b	Q9Y6B6	7.1	0.67	1.21	0.81
IPI00165164	Similar to ubiquitin-conjugating enzyme E2I	Q9BQ25	16.8	0.67	0.90	1.32
IPI00215719	60S ribosomal protein L18	Q07020	31	0.67	1.10	0.55
IPI00027463	Calcyclin	P06703	24.4	0.66	1.11	0.58
IPI00021828	Cystatin B	P04080	44.9	0.66	0.84	0.72
IPI00182728	SKD1 protein	O75351	8.2	0.66	0.93	1.24
IPI00008524	Polyadenylate-binding protein 1	P11940	23.3	0.66	0.97	0.56
IPI00216237	ribosomal protein L36	Q9Y3U8	14.3	0.66	1.04	0.80
IPI00219520	UNR protein	O75534	5.6	0.66	1.03	0.63
IPI00395748	Cytosolic acyl coenzyme A thioester hydrolase	O00154	14.8	0.65	1.04	0.84
IPI00186712	40S ribosomal protein S26	P02383	20.6	0.65	1.20	0.65
IPI00170935	Hypothetical protein KIAA1185	Q8N1G4	28.3	0.65	1.14	0.98
IPI00032826	Hsc70-interacting protein	P50502	13	0.65	1.02	0.60
IPI00220067	leucine aminopeptidase	P28838	8.1	0.65	0.80	0.87
IPI00215790	60S ribosomal protein L38	P23411	19.3	0.65	0.93	0.62
IPI00395865	Histone acetyltransferase type B subunit 2	Q16576	5	0.64	0.69	0.84
IPI00000861	LIM and SH3 domain protein 1	Q14847	9.2	0.64	0.71	0.48
IPI00165486	similar to ribosomal protein S2		9.6	0.63	0.93	0.28
IPI00184821	Bifunctional coenzyme A synthase (CoA synthase)	Q13057	11.7	0.63	0.45	1.26

IPI	ProteinName	Swiss-Prot	% Cov	OFF+T/OFF−T	ON−T/OFF−T	ON+T/OFF−T
IPI00217709	DNA topoisomerase II, beta isozyme	Q02880	6.2	0.63	1.08	1.00
IPI00018768	Translin	Q15631	5.3	0.63	0.99	0.71
IPI00011603	26S proteasome non-ATPase regulatory subunit 3	O43242	8.6	0.60	1.01	0.37
IPI00396417	MHC class I antigen	Q861B7	6.3	0.57	1.20	1.31
IPI00334922	Hypothetical protein FLJ10519	Q9NVT5	8.8	0.57	0.69	0.90
IPI00382700	Filamin B	O75369	7.1	0.55	0.90	0.66
IPI00296635	1,4-alpha-glucan branching enzyme	Q04446	2.5	0.52	0.97	0.69
IPI00219486	40S ribosomal protein S24	P16632	9.2	0.52	1.05	0.56
IPI00163230	COP9 signalosome subunit 6	O15387	12.8	0.52	0.59	0.60
IPI00303063	KIAA0648 protein	Q96DB6	8.9	0.51	0.92	0.78
IPI00382617	P37 AUF1	Q12771	11.5	0.50	0.77	0.71
IPI00384261	Muscleblind-like protein EP40s	Q86UV9	7.3	0.43	1.24	0.89
IPI00295386	carbonyl reductase 1	P16152	10.5	0.33	0.77	1.17
IPI00385399	mitogen-activated protein kinase 3	P27361	18.7	0.05	0.06	0.11
IPI00218547	Delta 1-pyrroline-5-carboylate synthetase	P54886	13	0.00	0.82	0.00
Proteins regulated upon inactivation of Nac1						
IPI00028481	Ras-related protein Rab-8	P24407	12.1	2.32	3.32	2.16
IPI00029079	GMP synthase [glutamine-hydrolyzing]	P49915	4.5	1.33	2.70	2.50
IPI00026087	Barrier-to-autointegration factor	O75531	15.7	1.84	2.47	
IPI00005270	Hypothetical protein	Q9BVD2	1.8	1.32	2.46	1.41
IPI00027192	Procollagen-lysine,2-oxoglutarate 5-dioxygenase 1	Q02809	3.9	1.77	2.10	0.84
IPI00218816	beta globin	P02023	19.7	1.81	2.10	2.49
IPI00259901	similar to peptidylprolyl isomerase A (cyclophilin A)	Q68J44	8.5	0.88	2.07	0.59
IPI00290416	Splice isoform 1 of Q9NTK5 Putative GTP-binding protein PTD004	Q9NTK5	9.1	1.17	1.92	1.02
IPI00382733	Transcription repressor	O75799	6.6	1.68	1.84	1.19
IPI00015953	Nucleolar RNA helicase II	Q9NR30	18.7	0.95	1.82	1.43
IPI00011937	Peroxiredoxin 4	Q13162	17.7	1.41	1.73	
IPI00215736	Alpha enolase	P06733	45	1.00	1.67	0.83
IPI00305185	Stromal cell protein	Q9BRV3	10.9	2.37	1.67	3.15
IPI00005648	Scaffold attachment factor B2	Q14151	5	1.13	1.67	1.25

IPI	ProteinName	Swiss-Prot	% Cov	OFF+T/OFF−T	ON−T/OFF−T	ON+T/OFF−T
IPI00003565	26S proteasome non-ATPase regulatory subunit 10	O75832	4	0.90	1.63	1.05
IPI00385566	Hypothetical protein FLJ30014	Q969M3	3.5	1.50	1.62	1.56
IPI00006865	Vesicle trafficking protein SEC22B	O75396	11.2	1.33	1.61	
IPI00016339	Ras-related protein Rab-5C	P51148	27.3	0.96	1.60	0.86
IPI00021383	Heterogeneous nuclear ribonucleoprotein A3	P51991	19	1.03	1.58	0.67
IPI00029485	Splice isoform p150 of Q14203 Dynactin 1	Q14203	5.8	1.07	1.56	
IPI00302925	T-complex protein 1, theta subunit	P50990	24.1	1.02	1.54	0.86
IPI00008918	Splice isoform Beta of Q9UHB6 Epithelial protein lost in neoplasm	Q9UHB6	7.2	0.98	1.52	0.64
IPI00016572	Small nuclear ribonucleoprotein G	Q15357	17.1	1.60	1.52	1.77
IPI00236879	Ataxin-2 related domain protein	Q8WWM7	7.1	1.74	1.51	1.84
IPI00301434	similar to My016 protein	Q9H3K6	13.8	1.03	1.51	
IPI00014238	Lysyl-tRNA synthetase	Q15046	6.7	1.50	1.49	
IPI00374657	vesicle-associated membrane protein-associated protein A isoform 1		4.9	1.74	1.49	0.97
IPI00176799	similar to hypothetical protein	Q8N3B3	12.2	1.04	1.48	0.88
IPI00299149	Ubiquitin-like protein SMT3B	P55855	32.6	1.83	1.48	1.08
IPI00005680	Hypothetical protein KIAA0095	Q14705	6.2	0.68	1.48	0.73
IPI00215802	Splice isoform Short of P23152 Splicing factor, arginine/serine- rich 3	P23152	29	0.79	1.44	0.81
IPI00009329	Utrophin	P46939	1.3	1.37	1.44	0.92
IPI00298971	Vitronectin (Serum spreading factor) (S-protein) (V75)	P04004	8.2	2.54	1.44	2.50
IPI00295589	Eukaryotic translation initiation factor 4GI	Q96I65	9.2	1.12	1.44	1.63
IPI00386621	Similar to calmodulin 2	Q9BRL5	16.3	1.36	1.44	1.10
IPI00025273	Splice isoform Long of P22102 Trifunctional purine biosynthetic pro	P22102	10.1	1.68	1.43	1.57
IPI00015947	DnaJ homolog subfamily B member 1	P25685	11.2	0.94	1.42	0.80
IPI00148062	Nuclear-associated protein SPAN-Xb	Q9NS25	43.7	1.25	1.42	1.36
IPI00382644	Putative eukaryotic translation initiation factor 1A	O75642	13.3	0.99	1.41	0.92
IPI00015786	Spectrin alpha chain, brain	Q13813	11.2	1.71	1.41	1.89
IPI00107357	Cleft lip and palate associated transmembrane protein 1	Q9BSS5	8.2	0.99	1.40	1.08
IPI00307162	VCL isoform meta-VCL	P18206	12.1	0.92	1.40	0.79
IPI00219156	ribosomal protein L30	P04645	10.4	0.83	1.39	1.13
IPI00168388	Splice isoform 1 of Q9UHB9 Signal recognition particle 68 kDa protein	Q9UHB9	9.3	1.15	1.39	1.23

IPI	ProteinName	Swiss-Prot	% Cov	OFF+T/OFF−T	ON−T/OFF−T	ON+T/OFF−T
IPI00021785	Cytochrome c oxidase polypeptide Vb, mitochondrial	P10606	25.6	1.31	1.38	2.03
IPI00220834	ATP-dependant DNA helicase II	P13010	13.3	1.34	1.38	0.91
IPI00017596	Microtubule-associated protein RP/EB family member 1	Q15691	10.4	0.97	1.37	0.96
IPI00006328	ATPase inhibitor, mitochondrial	Q9UII2	17.9	1.13	1.37	0.94
IPI00186711	Similar to plectin 1, intermediate filament binding protein, 500kD	Q96IE3	22.2	0.98	1.37	1.03
IPI00216393	Splice isoform Non-brain of P09496 Clathrin light chain A	P09496	9.6	1.37	1.37	1.09
IPI00293350	Translin-associated protein X	Q99598	5.5	1.05	1.36	1.17
IPI00008552	Thioredoxin-like protein 2	O76003	12.8	1.02	1.35	0.71
IPI00332570	Polyadenylate-binding protein 2	Q15097	9.2	1.01	1.34	1.27
IPI00218606	40S ribosomal protein S23	P39028	23.2	0.90	1.34	0.77
IPI00377199	Histone H2B.d	Q99877	48.7	1.01	1.34	0.99
IPI00304925	Heat shock 70 kDa protein 1	P08107	36.3	0.97	1.34	0.81
IPI00182373	Splice isoform IIa of O15460 Prolyl 4-hydroxylase alpha-2 subunit	O15460	9.8	0.97	1.34	0.70
IPI00084495	similar to ribosomal protein S15		18.3	1.09	1.33	1.19
IPI00217468	H1 histone family, member 5	P16401	19.5	0.98	1.33	0.68
IPI00383500	Splice isoform 2 of Q96AC1 Pleckstrin homology domain contain	Q96AC1	1.7	1.08	1.33	1.29
IPI00107117	Peptidylprolyl isomerase B	P23284	25.9	1.47	1.32	1.72
IPI00006558	CGI-61 protein	Q9NR47	10.1	1.67	1.32	0.75
IPI00297084	Dolichyl-diphosphooligosaccharide--protein glycosyltransferase 48 k	P39656	12.7	1.33	1.32	1.41
IPI00240812	Hypothetical protein KIAA0979	Q9Y2I5	7.4	0.85	1.32	0.71
IPI00376295	mitogen-activated protein kinase 1	P28482	13.9	0.95	1.32	1.22
IPI00396171	microtubule-associated protein 4 isoform 2	P27816-1	11.6	0.81	1.31	1.14
IPI00006482	Splice isoform Long of P05023 Sodium	P05023	10.8	1.31	1.31	1.33
IPI00026328	Thioredoxin-like protein p19	O95881	5.2	1.33	1.30	1.32
IPI00029557	GrpE protein homolog 1, mitochondrial	Q9HAV7	18.4	1.65	1.30	1.46
IPI00032313	Placental calcium-binding protein	P26447	29.7	1.08	0.69	0.87
IPI00395865	Histone acetyltransferase type B subunit 2	Q16576	5	0.64	0.69	0.84
IPI00005728	RER1 protein	O15258	7.7	1.09	0.69	0.94
IPI00334922	Hypothetical protein FLJ10519	Q9NVT5	8.8	0.57	0.69	0.90
IPI00019472	Neutral amino acid transporter B(0)	Q15758	6.7	1.55	0.68	1.19

IPI	ProteinName	Swiss-Prot	% Cov	OFF+T/OFF−T	ON−T/OFF−T	ON+T/OFF−T
IPI00017292	Splice isoform 1 of P35222 Beta-catenin	P35222	9.1	1.09	0.68	0.68
IPI00014197	Hypothetical protein	Q9UKY7	11.2	0.93	0.66	0.73
IPI00010810	Electron transfer flavoprotein alpha-subunit, mitochondrial	P13804	24.6	1.21	0.63	1.62
IPI00013068	Eukaryotic translation initiation factor 3 subunit 6	Q64252	4.5	0.85	0.63	1.01
IPI00396373	BLOCK 23	Q8NHW5	4.1	1.20	0.62	0.92
IPI00024364	Importin beta-2 subunit	Q92973	7.3	1.31	0.61	1.21
IPI00216298	thioredoxin	P10599	41	0.71	0.61	1.09
IPI00032406	DnaJ homolog subfamily A	O60884	5.3	0.76	0.60	0.78
IPI00163230	member 2 COP9 signalosome subunit 6	O15387	12.8	0.52	0.59	0.60
IPI00030940	Protein KIAA0052	P42285	2.6	0.74	0.59	1.18
IPI00154645	Similar to hypothetical protein FLJ12085	Q9HA83	2.3	0.94	0.57	0.92
IPI00395750	Splice isoform Long of O75083 WD-repeat protein 1	O75083	9.2	0.86	0.52	0.93
IPI00328193	Hypothetical protein	Q8WVM8	5.9	1.00	0.50	1.00
IPI00291005	cytosolic malate dehydrogenase	P40925	3.9	1.34	0.46	0.95
IPI00184821	Bifunctional coenzyme A synthase (CoA synthase) (NBP) (POV-2)	Q13057	11.7	0.63	0.45	1.26
IPI00219624	proteasome alpha 3 subunit isoform 1	P25788	4.7	1.29	0.45	1.22
IPI00219446	prostatic binding protein	P30086	20.3	0.68	0.43	0.54
IPI00385399	mitogen-activated protein kinase 3		18.7	0.05	0.06	0.11
IPI00334713	Splice isoform 3 of Q99729 Heterogeneous nuclear ribonucleoprotein A/B	Q99729	24.9	0.69	0.00	1.21
Proteins regulated upon paclitaxel treatment and induced N130 expression						
IPI00168812	Transmembrane receptor PTK7-4	Q8NFA6	7	1.07	0.72	6.54
IPI00305185	Stromal cell protein	Q9BRV3	10.9	2.37	1.67	3.15
IPI00328696	Hemoglobin alpha chain	P01922	17	2.45	1.20	2.78
IPI00329705	KIAA1363 protein	Q86WZ1	9.8	1.76	1.18	2.77
IPI00029079	GMP synthase [glutamine-hydrolyzing]	P49915	4.5	1.33	2.70	2.50
IPI00298971	Vitronectin (Serum spreading factor) (S-protein) (V75)	P04004	8.2	2.54	1.44	2.50
IPI00218816	beta globin	P02023	19.7	1.81	2.10	2.49
IPI00052229	Hypothetical protein	Q9UG74	6.7	0.68	0.98	2.48
IPI00160897	Hypothetical protein	Q969E5	37.6	2.05	1.08	2.27
IPI00005202	Membrane associated progesterone receptor component 2	O15173	10.3	1.59	1.14	2.17

IPI	ProteinName	Swiss-Prot	% Cov	OFF+T/OFF−T	ON−T/OFF−T	ON+T/OFF−T
IPI00028481	Ras-related protein Rab-8	P24407	12.1	2.32	3.32	2.16
IPI00030131	Splice isoform Beta of P42167 Thymopoietin, isoforms beta/gamma	P42167	14.1	1.81	1.23	2.11
IPI00016447	Hypothetical protein FLJ20502	Q9NX08	13.1	1.53	1.08	2.08
IPI00021785	Cytochrome c oxidase polypeptide Vb, mitochondrial	P10606	25.6	1.31	1.38	2.03
IPI00010157	S-adenosylmethionine synthetase gamma form	P31153	8.4	0.75	1.28	1.97
IPI00009407	Defender against cell death 1	P46966	14.2	1.39	1.13	1.94
IPI00026154	Protein kinase C substrate, 80 kDa protein, heavy chain	P14314	10.2	1.21	0.78	1.90
IPI00021187	RuvB-like 1	Q9Y265	10.1	1.04	1.29	1.89
IPI00015786	Spectrin alpha chain, brain	Q13813	11.2	1.71	1.41	1.89
IPI00395917	ferritin heavy chain	P02794	14.8	1.44	0.87	1.87
IPI00236879	Ataxin-2 related domain protein	Q8WWM7	7.1	1.74	1.51	1.84
IPI00377175	similar to Esterase D	Q9BVJ2	6.9	0.89	1.08	1.78
IPI00032825	Hypothetical protein CGI-109	Q9Y3B3	6.5	1.14	1.04	1.77
IPI00016572	Small nuclear ribonucleoprotein G	Q15357	17.1	1.60	1.52	1.77
IPI00027717	Component of gems 4	P57678	4.6	1.30	1.17	1.76
IPI00008453	Coronin 1C	Q9ULV4	10.1	1.07	1.28	1.75
IPI00017726	Splice isoform 1 of Q99714 3- hydroxyacyl-CoA dehydrogenase type II	Q99714	15.3	1.47	1.04	1.74
IPI00215916	cytochrome c	P00001	29.5	1.61	1.21	1.73
IPI00219291	Splice isoform 2 of P56134 ATP synthase f chain, mitochondrial	P56134	37.9	1.73	1.15	1.73
IPI00003927	40 kDa peptidyl-prolyl cis-trans isomerase	Q08752	3.5	1.02	1.09	1.73
IPI00216172	Splice isoform LAMP-2B of P13473 Lysosome-associated	P13473	4.9	1.29	1.18	1.73
IPI00107117	Peptidylprolyl isomerase B	P23284	25.9	1.47	1.32	1.72
IPI00011274	JKTBP2	O14979	18.8	1.05	1.20	1.69
IPI00021439	Actin, cytoplasmic 1	P02570	59.5	1.62	1.50	1.68
IPI00009236	Caveolin-1	Q03135	24.2	1.56	1.22	1.66
IPI00305064	Splice isoform CD44 of P16070 CD44 antigen	P16070	6.3	1.65	1.26	1.65
IPI00337814	Hypothetical protein	Q9BWL4	11.7	1.37	1.16	1.65
IPI00003965	Ubiquitin carboxyl-terminal hydrolase 7	Q93009	1.9	1.40	1.08	1.65
IPI00219835	Splice isoform Alpha-S1 of P04895 Guanine nucleotide-binding protein G(S),	P04895	23.9	1.55	1.06	1.64
IPI00295589	Eukaryotic translation initiation factor 4GI	Q96I65	9.2	1.12	1.44	1.63

IPI	ProteinName	Swiss-Prot	% Cov	OFF+T/OFF−T	ON−T/OFF−T	ON+T/OFF−T
IPI00396589	Interleukin enhancer binding factor 2, 45kD	Q9BWD4	19.2	2.01	0.88	1.63
IPI00010810	Electron transfer flavoprotein alpha-subunit, mitochondrial	P13804	24.6	1.21	0.63	1.62
IPI00165092	Hypothetical protein FLJ13995	Q9H817	6.3	1.37	0.87	1.61
IPI00011229	Cathepsin D	P07339	14.1	1.66	1.02	1.61
IPI00303882	Splice isoform B of O60664 Cargo selection protein TIP47	O60664	27.2	1.41	1.26	1.60
IPI00249267	similar to H2A histone family, member Z		39.1	1.05	0.91	1.57
IPI00025273	Splice isoform Long of P22102 Trifunctional purine biosynthetic protein adenosine-3	P22102	10.1	1.68	1.43	1.57
IPI00218019	Basigin long isoform	Q8IZL7	9.6	1.59	0.84	1.57
IPI00385566	Hypothetical protein FLJ30014	Q969M3	3.5	1.50	1.62	1.56
IPI00385098	MSTP086	Q7Z4F2	7.1	0.83	0.99	1.54
IPI00027252	repressor of estrogen receptor activity	Q9BXV3	15.1	1.31	0.96	1.54
IPI00291006	Malate dehydrogenase, mitochondrial	P40926	26.9	1.28	1.00	1.54
IPI00031479	Protein disulfide isomerase A5	Q14554	2.3	1.43	0.88	1.54
IPI00395769	ATP synthase gamma chain, mitochondrial	P36542	14	1.15	1.15	1.54
IPI00217952	Splice isoform 1 of Q06210	Q06210	8.6	1.51	0.96	1.52
IPI00329629	Glucosamine--fructose-6-phosphate DnaJ homolog subfamily C member 7	Q99615	5.3	0.86	0.72	1.50
IPI00003833	HSPC032	Q9Y6C9	16.8	0.83	1.26	1.49
IPI00297982	eukaryotic translation initiation factor 2, subunit 3 gamma, 52kDa	P41091	21.8	1.20	1.20	1.49
IPI00220985	Keratin, type I cytoskeletal 18	P05783	39.6	1.46	0.94	1.49
IPI00025095	Cellular nucleic acid binding protein	P20694	8.5	1.14	1.15	1.49
IPI00025874	Dolichyl-diphosphooligosaccharide--protein glycosyltransferase 67 kDa subunit	P04843	15.7	1.65	1.20	1.48
IPI00142634	Tubulin beta-5 chain	P05218	43	1.47	1.00	1.47
IPI00007188	ADP, ATP carrier protein, fibroblast isoform	P05141	46.6	1.24	0.94	1.46
IPI00026167	NHP2-like protein 1	P55769	24.2	1.37	0.86	1.46
IPI00029557	GrpE protein homolog 1, mitochondrial	Q9HAV7	18.4	1.65	1.30	1.46
IPI00164305	Membrane associated protein SLP-2	Q9UJZ1	11.8	1.24	1.10	1.45
IPI00293102	Splice isoform 2 of Q15257 Protein phosphatase 2A, regulatory subunit B′	Q15257	12.8	1.33	1.05	1.45
IPI00015148	Ras-related protein Rap-1b	P09526	14.7	1.61	1.11	1.44
IPI00003519	116 kDa U5 small nuclear ribonucleoprotein component	Q15029	7.2	1.17	0.83	1.44

IPI	ProteinName	Swiss-Prot	% Cov	OFF+T/OFF−T	ON−T/OFF−T	ON+T/OFF−T
IPI00176903	Leucine-zipper protein FKSG13	O00535	15.9	1.14	1.08	1.44
IPI00021954	Golgi-specific brefeldin A-resistance guanine nucleotide exchange factor 1	Q92538	7	1.37	0.87	1.43
IPI00015953	Nucleolar RNA helicase II	Q9NR30	18.7	0.95	1.82	1.43
IPI00171626	hypothetical protein FLJ12443	Q7Z4G6	9.9	1.28	0.99	1.43
IPI00009922	DC50	Q9GZT3	12.8	1.33	1.01	1.42
IPI00220855	Similar to H2A histone family, member O	Q9BTM1	58.9	1.33	0.89	1.42
IPI00220739	progesterone receptor membrane component 1	O00264	16.9	1.52	1.08	1.42
IPI00290142	CTP synthase	P17812	12.5	1.33	1.10	1.42
IPI00297084	Dolichyl-diphosphooligosaccharide--protein glycosyltransferase 48 kDa subunit	P39656	12.7	1.33	1.32	1.41
IPI00005270	Hypothetical protein	Q9BVD2	1.8	1.32	2.46	1.41
IPI00019927	26S proteasome non-ATPase regulatory subunit 7	P51665	11.4	1.25	1.17	1.41
IPI00333010	SR-related CTD associated factor 6	Q8WU30	8	1.18	1.03	1.40
IPI00028091	Actin-like protein 3	P32391	6.7	0.80	1.16	1.40
IPI00386685	citrate synthase isoform a	Q96FZ8	17	1.24	1.06	1.40
IPI00007824	ABP125	Q9UM06	4.2	1.08	0.78	1.40
IPI00219219	beta-galactosidase binding lectin	P09382	65.2	1.81	1.14	1.39
IPI00021440	Actin, cytoplasmic 2	P02571	59.5	1.27	0.48	1.39
IPI00024919	Thioredoxin-dependent peroxide reductase, mitochondrial	P30048	25.4	1.40	1.05	1.39
IPI00020984	Calnexin	P27824	17.1	1.29	1.09	1.38
IPI00386803	LIM and SH3 protein 1	Q96IG0	10.2	1.16	1.02	1.38
IPI00012578	Importin alpha-4 subunit	O00629	13.4	1.24	0.96	1.37
IPI00215918	ADP-ribosylation factor 4	P18085	22.2	1.17	0.81	1.37
IPI00019345	Ras-related protein Rap-1A	P10113	14.7	1.21	0.75	1.37
IPI00023542	gp25L2 protein	Q9BVK6	20.9	1.23	1.12	1.37
IPI00009328	Probable ATP-dependent helicase DDX48	P38919	15.8	1.10	1.01	1.37
IPI00291467	ADP, ATP carrier protein, liver isoform T2	P12236	44.3	1.29	1.00	1.36
IPI00219604	mitogen-activated protein kinase kinase 1	Q02750	7.6	1.39	0.99	1.36
IPI00009342	Ras GTPase-activating-like protein IQGAP1	P46940	11.9	1.08	0.95	1.36
IPI00027493	4F2 cell-surface antigen heavy chain	P08195	22.9	1.37	0.97	1.36
IPI00333383	Adapter-related protein complex 2 beta 1 subunit	P21851	2.8	1.13	1.09	1.36

IPI	ProteinName	Swiss-Prot	% Cov	OFF+T/OFF−T	ON−T/OFF−T	ON+T/OFF−T
IPI00148062	Nuclear-associated protein SPAN-Xb	Q9NS25	43.7	1.25	1.42	1.36
IPI00396304	tubulin, alpha, ubiquitous	P68363	39.7	1.27	0.88	1.36
IPI00034283	Similar to tubulin, beta, 4	Q9BUF5	34.8	1.07	1.12	1.35
IPI00018206	Aspartate aminotransferase, mitochondrial	P00505	8.6	1.00	0.79	1.35
IPI00002134	26S proteasome non-ATPase regulatory subunit 5	Q16401	19.4	1.23	1.25	1.35
IPI00022793	Trifunctional enzyme beta subunit, mitochondrial (TP- beta)	P55084	13.5	1.30	1.29	1.35
IPI00216492	Splice isoform 2 of P31942 Heterogeneous nuclear ribonucleoprotein H3	P31942	8.2	1.55	1.14	1.35
IPI00002520	Serine hydroxymethyltransferase, mitochondrial	P34897	12.5	1.79	1.13	1.34
IPI00221012	Splice isoform Long of Q93008 Probable ubiquitin carboxyl-terminal hydrolase FAF-X	Q93008	6.1	1.11	1.02	1.34
IPI00217466	H1 histone family, member 3	P16402	29	1.18	0.98	1.34
IPI00216312	vimentin	P08670	53.4	1.25	1.15	1.34
IPI00215914	ADP-ribosylation factor 1	P32889	47.5	1.00	0.89	1.33
IPI00046828	similar to CG15881-PB	Q4VC31	14.5	1.37		1.33
IPI00026111	Hypothetical protein	Q9BZS3	14.3	1.15	1.03	1.33
IPI00016638	ATP synthase alpha chain, mitochondrial	P25705	18.1	1.21	0.95	1.33
IPI00215920	ADP-ribosylation factor 6	P26438	10.9	1.00	1.13	1.33
IPI00218889	Splice isoform 2 of P50570 Dynamin 2	P50570	8.7	1.23	0.95	1.33
IPI00218343	Tubulin alpha-6 chain	Q9BQE3	59.8	1.25	0.95	1.33
IPI00006482	Splice isoform Long of P05023	P05023	10.8	1.31	1.31	1.33
IPI00165164	Sodium/Similar to ubiquitin-conjugating enzyme E2I	Q9BQ25	16.8	0.67	0.90	1.32
IPI00185600	Annexin A11	P50995	8.3	0.85	0.74	1.32
IPI00021766	Splice isoform 1 of Q9NQC3 Reticulon 4	Q9NQC3	7.1	1.41	1.09	1.32
IPI00028055	Transmembrane protein Tmp21	P49755	22.4	1.41	1.11	1.32
IPI00026328	Thioredoxin-like protein p19	O95881	5.2	1.33	1.30	1.32
IPI00220362	10 kDa heat shock protein, mitochondrial	Q04984	14.2	1.14	1.07	1.32
IPI00008708	PBK1 protein	Q8WUZ1	8.3	1.00	1.07	1.32
IPI00306667	Splice isoform CNPII of P09543 2′,3′-cyclic nucleotide 3′-phosphodiesterase	P09543	4.1	0.99	1.13	1.31
IPI00329351	60 kDa heat shock protein, mitochondrial	P10809	31	1.33	1.05	1.31
IPI00027230	Endoplasmin	P14625	22.4	1.21	1.04	1.31

IPI	ProteinName	Swiss-Prot	% Cov	OFF+T/OFF−T	ON−T/OFF−T	ON+T/OFF−T
IPI00004968	Nuclear matrix protein NMP200	Q9UMS4	6.9	1.20	0.98	1.31
IPI00396417	MHC class I antigen	Q861B7	6.3	0.57	1.20	1.31
IPI00215884	splicing factor, arginine/serine-rich 1 (splicing factor 2, alternate splicing factor)	Q07955	27	1.18	1.11	1.30
IPI00186338	unnamed protein		41.9	1.33	1.09	1.30
IPI00374260	ribosomal protein L10	P27635	30.4	0.68	0.98	0.69
IPI00296635	1,4-alpha-glucan branching enzyme	Q04446	2.5	0.52	0.97	0.69
IPI00027681	Nicotinamide N-methyltransferase	P40261	13.3	0.82	0.89	0.69
IPI00217468	H1 histone family, member 5	P16401	21.2	0.98	1.33	0.68
IPI00021840	40S ribosomal protein S6	P10660	23.3	0.75	1.04	0.68
IPI00017292	Splice isoform 1 of P35222 Beta-catenin	P35222	9.1	1.09	0.68	0.68
IPI00021383	Heterogeneous nuclear ribonucleoprotein A3	P51991	19	1.03	1.58	0.67
IPI00386590	DJ423B22.4 (Ribosomal protein S27	Q9BQZ7	13.1	0.90	1.19	0.66
IPI00382700	Splice isoform 6 of O75369 Filamin B	O75369	7.1	0.55	0.90	0.66
IPI00396660	Elongation factor 1-beta	P24534	17.4	0.93	1.17	0.66
IPI00014808	Platelet-activating factor acetylhydrolase IB gamma subunit	Q15102	27.3	0.92	0.93	0.66
IPI00219757	Glutathione S-transferase P	P09211	31.5	0.73	0.92	0.65
IPI00186712	40S ribosomal protein S26	P02383	20.6	0.65	1.20	0.65
IPI00015952	Eukaryotic translation initiation factor 4 gamma 2	P78344	5.6	0.71	1.13	0.65
IPI00216320	Splice isoform 2 of O00764 Pyridoxal kinase	O00764	14.8	0.88	0.93	0.64
IPI00217223	Multifunctional protein ADE2 [Includes:	P22234	9.8	0.74	0.75	0.64
IPI00025019	Proteasome subunit beta type 1	P20618	15.8	1.52	1.00	0.64
IPI00386491	Splice isoform Short of Q00839 Heterogenous nuclear ribonucleoprotein U	Q00839	21	0.72	0.94	0.64
IPI00008918	Splice isoform Beta of Q9UHB6 Epithelial protein lost in neoplasm	Q9UHB6	7.2	0.98	1.52	0.64
IPI00332371	6-phosphofructokinase, liver type	P17858	16.5	0.70	0.81	0.63
IPI00219520	Splice isoform Short of O75534 UNR protein	O75534	5.6	0.66	1.03	0.63
IPI00033904	similar to ribosomal protein S3a	P61247	26.5	0.69	1.03	0.63
IPI00013184	N-terminal acetyltransferase complex ARD1 subunit homolog	P41227	4.7	1.13	1.15	0.63
IPI00336008	aldehyde dehydrogenase 5A1 isoform 1	Q8N3W7	8.2	1.22	1.12	0.62
IPI00215790	60S ribosomal protein L38	P23411	19.3	0.65	0.93	0.62
IPI00000874	Peroxiredoxin 1	Q06830	41.2	0.81	1.00	0.62

IPI	ProteinName	Swiss-Prot	% Cov	OFF+T/OFF−T	ON−T/OFF−T	ON+T/OFF−T
IPI00018219	Transforming growth factor-beta induced protein IG-H3	Q15582	7.2	0.96	0.81	0.60
IPI00032826	Hsc70-interacting protein	P50502	13	0.65	1.02	0.60
IPI00163230	COP9 signalosome subunit 6	O15387	12.8	0.52	0.59	0.60
IPI00000051	Prefoldin subunit 1	O60925	23.8	0.81	1.17	0.59
IPI00259901	similar to peptidylprolyl isomerase A (cyclophilin A)	Q68J44	8.5	0.88	2.07	0.59
IPI00027463	Calcyclin	P06703	24.4	0.66	1.11	0.58
IPI00374119	smooth muscle and non-muscle myosin alkali light chain isoform 3		33.8	0.72	1.09	0.58
IPI00025512	Heat shock 27 kDa protein	P04792	38.5	0.73	0.87	0.57
IPI00302850	Small nuclear ribonucleoprotein Sm D1	P13641	31.5	0.84	0.85	0.57
IPI00008524	Polyadenylate-binding protein 1	P11940	23.3	0.66	0.97	0.56
IPI00219486	Splice isoform 2 of P16632 40S ribosomal protein S24	P16632	9.2	0.52	1.05	0.56
IPI00004656	Beta-2-microglobulin	P01884	21.8	0.84	0.73	0.55
IPI00215719	60S ribosomal protein L18	Q07020	31	0.67	1.10	0.55
IPI00219446	prostatic binding protein	P30086	20.3	0.68	0.43	0.54
IPI00219158	ribosomal protein L29	P47914	30.8	0.69	1.17	0.53
IPI00375511	Similar to RIKEN cDNA 2510008H07 gene	Q8N6E1	21.5	0.77	1.15	0.50
IPI00000861	LIM and SH3 domain protein 1	Q14847	9.2	0.64	0.71	0.48
IPI00026271	40S ribosomal protein S14	P06366	24.5	0.73	1.13	0.47
IPI00011603	26S proteasome non-ATPase regulatory subunit 3	O43242	8.6	0.60	1.01	0.37
IPI00165486	similar to ribosomal protein S2		9.6	0.63	0.93	0.28
IPI00021700	Proliferating cell nuclear antigen	P12004	8.8	0.72	1.26	0.19
IPI00385399	mitogen-activated protein kinase 3	P27361	18.7	0.05	0.06	0.11
IPI00218547	Delta 1-pyrroline-5-carboxylate synthetase (P5CS)	P54886	4.7	0.00	0.82	0.00

Table 3

Mitochondrial protein changes related to paclitaxel quantified by iTRAQ were also measured by label-free quantitation methods

IPI	ProteinName	Swiss-Prot	methods	OFF+T/OFF−T	ON−T/OFF−T	ON+T/OFF−T
IPI00002520	Serine hydroxymethyltransferase, mitochondrial	P34897	iTRAQ	1.79	1.13	1.34
IPI00219291	ATP synthase f chain, mitochondrial	P56134	iTRAQ	1.73	1.15	1.73
			LC-MS	1.70	1.16	1.99
IPI00029557	GrpE protein homolog 1, mitochondrial	Q9HAV7	iTRAQ	1.65	1.30	1.46
IPI00009960	Mitochondrial inner membrane protein	Q16891	iTRAQ	1.64	1.20	1.05
IPI00215916	cytochrome c	P00001	iTRAQ	1.61	1.21	1.73
			LC-MS	1.19	1.00	1.27
IPI00031522	Trifunctional enzyme alpha subunit, mitochondrial	P40939	iTRAQ	1.55	0.80	1.19
			SC	3.01	3.00	6.06
IPI00014230	Complement component 1, mitochondrial	Q07021	iTRAQ	1.47	1.17	1.25
			SC	1.59	0.60	0.40
IPI00024919	Thioredoxin-dependent peroxide reductase, mitochondrial	P30048	iTRAQ	1.40	1.05	1.39
			SC	1.25	0.50	1.00
IPI00024993	Enoyl-CoA hydratase, mitochondrial	P30084	iTRAQ	1.38	0.81	1.12
			SC	1.67	1.33	1.33
IPI00329351	60 kDa heat shock protein, mitochondrial	P10809	iTRAQ	1.33	1.05	1.31
IPI00007765	Stress-70 protein, mitochondrial	P38646	iTRAQ	1.33	1.05	1.12
			LC-MS	1.71	1.21	1.47
			SC	1.75	1.50	1.65
IPI00021785	Cytochrome c oxidase polypeptide Vb, mitochondrial	P10606	iTRAQ	1.31	1.38	2.03
IPI00304802	Dihydrolipoamide succinyltransferase component of 2-oxoglutarate dehydrogenase complex, mitochondrial	P36957	iTRAQ	1.31	0.92	1.23
IPI00022793	Trifunctional enzyme beta subunit, mitochondrial	P55084	iTRAQ	1.30	1.29	1.35

Proteomics Clin Appl. Author manuscript; available in PMC 2010 November 22.